Instituto de Investigaciones en Matemáticas Aplicadas y en Sistemas

A chemotactic model of bacterial aggregation with nonlinear cross diffusion

Ramón G. Plaza
Institute of Applied Mathematics (IIMAS),
National Autonomous University of Mexico (UNAM)

Joint work with:

- Carlos Málaga (Physics Dept., UNAM)
- Juan Francisco Leyva

Bacterial aggregation patterns

- Bacterial colonies *in vitro* exhibit morphological aggregation patterns
- Hostile environmental conditions: low nutrient level, hard agar
- Adaptive survival strategies lead to complex spatio-temporal patterns.
- Complex patterns; complex self-organization: micro-level (cell-cell), macro-level (colony), chemical signalling, gene exchange.
- Example: *Bacillus subtilis*. Gram + bacteria, resistant.

Observations

- Low nutrient, hard agar: Diffusion limited aggregation (DLA). Fractal patterns (Matsuyama and Matsushita (1993); Ben-Jacob (1994). **(A)**
- Semi-solid agar, low nutrient: Dense branch morphology (DBM). Smooth colony envelope (Ohgiwari et al. (1992)). **(E)**
- Higher nutrient, soft agar: homogeneous colony, smooth boundary envelope. **(D)**
- Hard agar, high nutrient: envelope with fractal boundary. **(B)**
- Rings: transition from **(B)** to **(D)**.

C_n - concentration of nutrient; C_a - agar concentration (softness $1/C_a$)

Morphological diagram

Rings (C) Fractal (A)

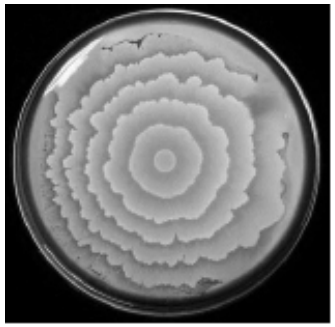

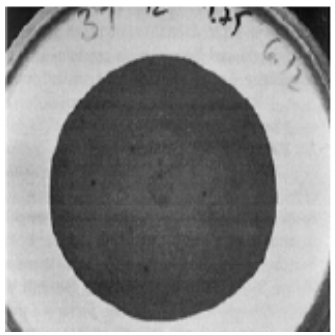

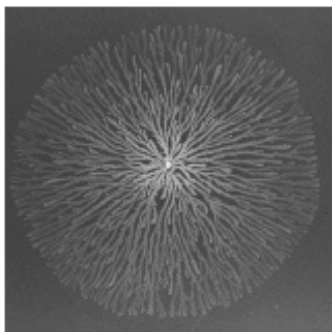

Disk (D) DBM (E)

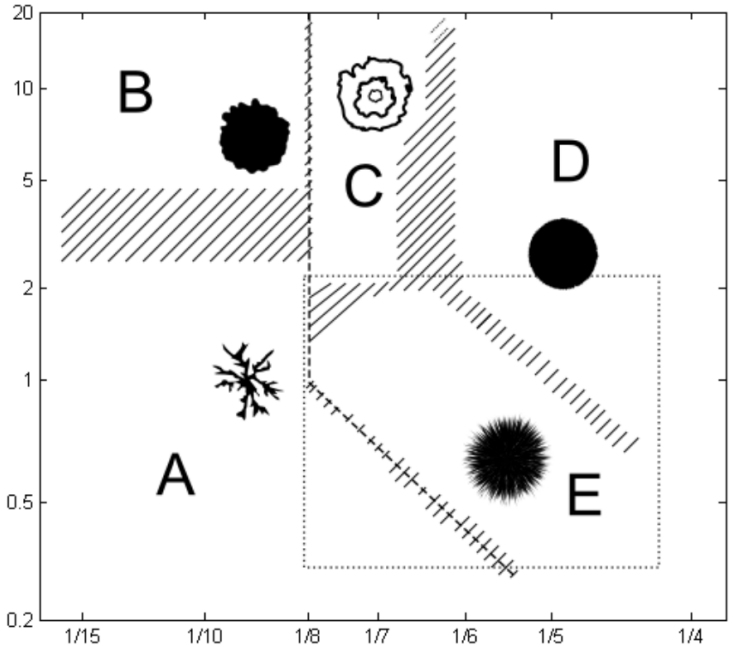

C_n vs. $1/C_a$

Deterministic reaction-diffusion models

- Continuous time evolution systems of PDEs
- Reaction-diffusion modelling (Murray)
- Non-equilibrium patterns: colonies in invaded and non-invading regions
- Diffusive growth: the boundary of the colony is unstable
- Traveling wave approximations, speed of colony envelope.
- Toy model (paradigm): Fisher-KPP one -d reaction-diffusion equations (propagating front)
- Other patterns: Turing diffusion-driven linear instability

Kawasaki's model

Kawasaki et al. *J. Theor. Biol.* **188** (1997): Non-linear cross-diffusion model

$$\begin{aligned} n_t &= D_n \Delta n - f(n,b) \\ b_t &= \nabla \cdot (D_b \nabla b) + \theta f(n,b) \end{aligned} \tag{K}$$

n - nutrient and b - bacterial concentrations, $(x,y) \in \Omega \subset \mathbb{R}^2$, $t > 0$. Diffusion: $D_n > 0$ constant.

Consumption rate: $f(n,b)$, $\theta > 0$ -conversion rate factor.

No-flux boundary conditions.

Nonlinear cross-diffusion

$$D_b = \sigma n b$$

$\sigma = \sigma_0(1+\Delta)$. $\sigma_0 \sim 1/C_a$. Δ - random parameter

Features:

- Ohgiwari et al., (1992): low and intermediate C_a, growth by mov. cells. Low agar. Boundary front: cells are active on the bdry. *only*.
- Kawasaki: immotility when either n *or* b are low.
- Complex dense morphology. Rich mathematical structure (Murray; Satnoianu, Maini and Sánchez-Garduño (2001); Sherratt (2010)).

Nonlinear cross-diffusion

$$D_b = \sigma n b$$

$\sigma = \sigma_0(1+\Delta)$. $\sigma_0 \sim 1/C_a$. Δ - random parameter

Features:

- Ohgiwari et al., (1992): low and intermediate C_a, growth by mov. cells. Low agar. Boundary front: cells are active on the bdry. *only*.
- Kawasaki: immotility when either n *or* b are low.
- Complex dense morphology. Rich mathematical structure (Murray; Satnoianu, Maini and Sánchez-Garduño (2001); Sherratt (2010)).

Chemotaxis

E. Ben-Jacob's group (Univ. of Tel-Aviv):

- Ben-Jacob et al. *Nature* **368** (1994): Experimental evidence of chemotaxis towards amino acids (nutrients)
- Golding et al. *Phys. A* **260** (1997): Role of chemotaxis in the formation of patterns; theoretical and experimental arguments
- Ben-Jacob et al. *Adv. Phys.* **49** (2000): Identified three types of chemotactic internal signalling. Propose, based on experiments, a relation bet. diffusion and chemotaxis (certain nutrient regimes)

Chemotactic responses:

- (Repulsive - Long range) By starving bacteria in the center.
- (Attractive - Short range) Bacteria in the front ask for help to metabolize waste.
- **Nutrient chemotaxis:** Dominant signal. Attractive, short range.

Chemotactic flux

$$J_c = \xi(b)\chi(n)\nabla n.$$

$\chi = \chi(n) > 0$ - chemotactic sensitivity function
$\xi = \xi(b)$ - bacterial response function to nutrient gradient

- $\xi > 0$ - attractive
- $\xi < 0$ - repulsive

Receptor's law

Lapidus-Schiller (1976):

$$\chi(n) = \frac{\chi_0 K_d}{(K_d + n)^2}$$

- $\chi_0 > 0$: constant (strength of the chemotaxis)
- $K_d > 0$: receptor-ligand binding dissociation constant. Units of n; concentration 1/2 of receptor to be occupied. Unique value under fixed conditions.

First approximation: n small, $\chi(n) \sim \chi_0 / K_d$.

Ben-Jacob's conjecture

In semi-solid agar, low colony density:

$$|\xi(b)| \propto bD_b.$$

Examples:

- Keller-Segel (1971): $D_b > 0$ constant $\Rightarrow$ $\xi(b) = \pm bD_b$.
- Kitsunezaki (1997): $D_b = D_0 b^m$, $m > 0$, $D_0 > 0$ const. $\Rightarrow \xi(b) = bD_b = D_0 b^{m+1}$

Ben-Jacob's conjecture

In semi-solid agar, low colony density:

$$|\xi(b)| \propto bD_b.$$

Examples:

- Keller-Segel (1971): $D_b > 0$ constant $\Rightarrow$ $\xi(b) = \pm bD_b$.
- Kitsunezaki (1997): $D_b = D_0 b^m$, $m > 0$, $D_0 > 0$ const. $\Rightarrow \xi(b) = bD_b = D_0 b^{m+1}$

Chemotactic flux

$$D_b = \sigma n b$$

$$J_c = \sigma n b^2 \chi(n) \nabla n,$$

Positive (attractive) bacterial response function. χ is either constant or the Lapidus-Schiller receptor law.

Chemotactic model with nonlinear cross diffusion

With receptor's law:

$$n_t = D_n \Delta n - \kappa n b,$$

$$b_t = \nabla \cdot (\sigma n b \nabla b) + \theta \kappa n b - \nabla \cdot \left(\sigma n b^2 \frac{\chi_0 K_d}{(K_d + n)^2} \nabla n \right),$$

$(x,y) \in \Omega \subset \mathbb{R}^2$, $t \geq 0$. $\sigma = \sigma_0(1+\Delta)$.

- No-flux boundary conditions

$$\nabla b \cdot \nu = 0, \quad \nabla n \cdot \nu = 0, \qquad (x,y) \in \partial\Omega$$

- Initial conditions

$$n(x,y,0) = \hat{n}_0, \quad b(x,y,0) = \hat{b}_0(x,y)$$

$\hat{n}_0 > 0$ constant, $\hat{b}_0$ given.

Non-dimensionalization

$$\tilde{x} = \left(\frac{\theta K_d \kappa}{D_n}\right)^{1/2} x, \quad \tilde{y} = \left(\frac{\theta K_d \kappa}{D_n}\right)^{1/2} y, \quad \tilde{t} = (\theta K_d \kappa) t,$$

$$\tilde{n} = \frac{n}{K_d}, \quad \tilde{b} = \frac{b}{\theta K_d}, \quad \tilde{\sigma} = \left(\frac{\theta K_d^2}{D_n}\right)\sigma.$$

$$n(x,y,0) = \hat{n}_0/K_d \equiv n_0,$$
$$b(x,y,0) = \hat{b}_0(x,y,0)/(\theta K_d) \equiv b_0(x,y,0),$$

$$n_t = \Delta n - nb,$$

$$b_t = \nabla \cdot (\sigma nb \nabla b) + nb - \chi_0 \nabla \cdot \left(\frac{\sigma nb^2}{(1+n)^2} \nabla n \right). \qquad \text{(C)}$$

Initial cond. $n(x,y,0) = n_0$, $b(x,y,0) = b_0(x,y)$. No flux b.c.

Free parameters:

- $\sigma_0 > 0$ - hardness of the agar medium (large σ_0, soft agar)
- $n_0 > 0$ - relative initial nutrient
- $\chi_0 \geq 0$ - intensity of the chemotaxis

$$n_t = \Delta n - nb,$$
$$b_t = \nabla \cdot (\sigma nb \nabla b) + nb - \chi_0 \nabla \cdot \left(\frac{\sigma nb^2}{(1+n)^2} \nabla n \right). \qquad \text{(C)}$$

Initial cond. $n(x,y,0) = n_0$, $b(x,y,0) = b_0(x,y)$. No flux b.c.

Free parameters:

- $\sigma_0 > 0$ - hardness of the agar medium (large σ_0, soft agar)
- $n_0 > 0$ - relative initial nutrient
- $\chi_0 \geq 0$ - intensity of the chemotaxis

Approximation:

- Conservation law: $b + n \approx C$ constant.
- $n = n_0 - b$ leads to a logistic equation, absence of diffusion and chemotaxis
- $\chi(n) \approx \chi_0$
- $\sigma = \sigma_0$

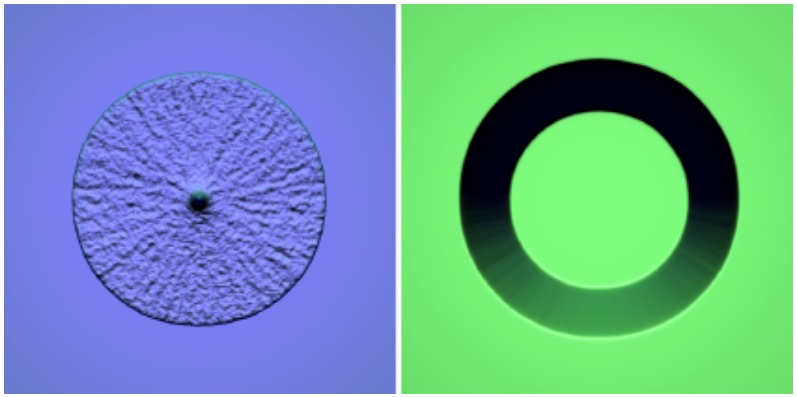

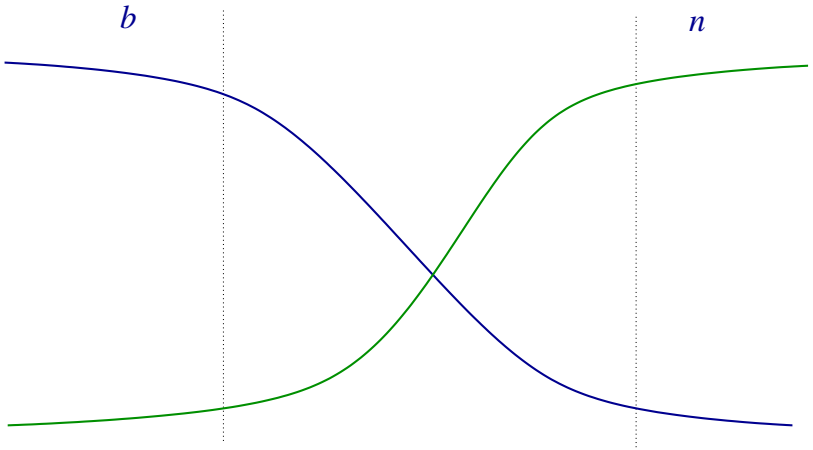

Front approximation: $n \approx n_0 - b$

Approximate scalar equation near front:

$$b_t = \sigma_0 \nabla \cdot (\tilde{D}(b, \chi_0) \nabla b) + g(b)$$

$$\tilde{D}(b, \chi_0) = n_0 b \left(1 - \frac{b}{n_0}\right)(1 + \chi_0 b)$$

$$g(b) = n_0 b \left(1 - \frac{b}{n_0}\right)$$

- Scalar equation for b with Fisher-type reaction term $g(b)$
- Effective non-linear diffusion coefficient $\tilde{D}(b, \chi_0)$

Geometric front propagation

- Local curvilinear coordinates: normal $\zeta(x,y,t)$, tangent $\tau(x,y,t)$
- $b(x,y,t) \approx b(\zeta(x,y,t))$ motion in the normal direction

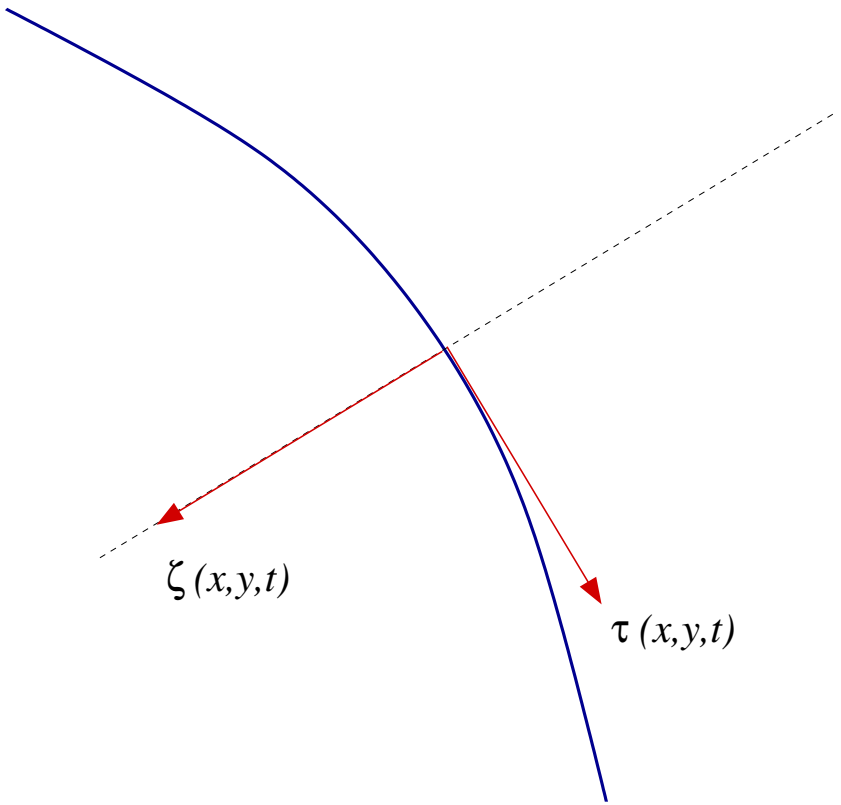

Front equation

$$-cb' = \sigma_0(\tilde{D}(b)b')' + b(n_0 - b)$$

$$c = -\zeta_t + \sigma_0\tilde{D}(b)\Delta\zeta$$

Theoretical results

- Malaguti and Marcelli, *J. Diff Equations* **195** (2003)

Fisher-KPP equation with doubly degenerate diffusion:

$$u_t = (D(u)u_x)_x + g(u)$$

$$0 < u < 1,\ D \in C^1([0,1]),\ g \in C^1([0,1])$$

$$D(0) = D(1) = 0, \qquad D(u) > 0 \ \text{ for all } \ 0 < u < 1,$$

$$g(0) = g(1) = 0, \qquad g(u) > 0 \ \text{ for all } \ 0 < u < 1,$$

Existence of TWS provided the speed c satisfies:

$$0 < c_* \leq c$$

Threshold velocity c_* of a sharp front:

$$0 < c_* \leq 2\sqrt{\sup_{s\in(0,1)} \frac{D(s)g(s)}{s}}.$$

Front equation:

$$b_t = (\tilde{D}(b,\chi_0)b_x)_x + g(b),$$

$b \in [0,n_0]$, $\tilde{D}(b,\chi_0)$, $g(b)$ chemotactic dependent $\chi_0 \geq 0$.
Existence of TWS linked to the solution to the b.v. problem:

$$\frac{dz}{db} = -c - \frac{\tilde{D}(b,\chi_0)g(b)}{z},$$
$$z(0^+) = z(n_0^-) = 0.$$

$$A_{\chi_0} = \{c > 0 : \text{b.v. problem has a non-positive solution}\}.$$

$$c_* = \inf A_{\chi_0}$$

Lemma

For any fixed value of $n_0 > 0$ and for all values of $\chi_0 \geq 0$ there hold,

(i) $\bar{c}(\chi_0) \geq \bar{c}(0)$, *and*

(ii) $c_*(\chi_0) \geq c_*(0)$

where

$$\bar{c}(n_0, \chi_0) = 2n_0\sqrt{\sigma_0}\sqrt{\max_{b\in[0,n_0]} b\left(1-\frac{b}{n_0}\right)^2(1+\chi_0 b)}.$$

Let

$$\psi(b) = b(1-b/n_0)^2(1+\chi_0 b) \geq 0$$

for $b \in [0, n_0]$, each $\chi_0 \geq 0$. Global max:

$$\psi_{\max} = \psi(b_*),$$

$$b_* = \frac{1}{2}\left(\frac{n_0}{2} - \frac{3}{4\chi_0}\right) + \frac{1}{2}\sqrt{\left(\frac{n_0}{2} - \frac{3}{4\chi_0}\right)^2 + \frac{n_0}{\chi_0}} \in (0, n_0).$$

$$\bar{c}(n_0, \chi_0) = 2n_0\sqrt{\sigma_0}\sqrt{\psi(b_*)}.$$

Let

$$\psi(b) = b(1-b/n_0)^2(1+\chi_0 b) \geq 0$$

for $b \in [0, n_0]$, each $\chi_0 \geq 0$. Global max:

$$\psi_{\max} = \psi(b_*),$$

$$b_* = \frac{1}{2}\left(\frac{n_0}{2} - \frac{3}{4\chi_0}\right) + \frac{1}{2}\sqrt{\left(\frac{n_0}{2} - \frac{3}{4\chi_0}\right)^2 + \frac{n_0}{\chi_0}} \in (0, n_0).$$

$$\bar{c}(n_0, \chi_0) = 2n_0\sqrt{\sigma_0}\sqrt{\psi(b_*)}.$$

No chemotaxis $\chi_0 = 0$: Newman (1980), $\psi_{\max} = 4n_0/27$

$$\bar{c}(n_0, 0) = 2n_0\sqrt{\sigma_0}\sqrt{\frac{4n_0}{27}} = \frac{4}{3\sqrt{3}} n_0^{3/2}\sigma^{1/2}$$

Bounds for the speed of the sharp front. In the approximation $\kappa = -\Delta\zeta > 0$ (curvature), so that

$$s = -\zeta_t \geq c_*(\chi_0) + \sigma_0\tilde{D}(b)\kappa > 0.$$

Approximate interface equation of motion with chemotactic contribution:

$$s = -\zeta_t \geq c_*(\chi_0) + \sigma_0\tilde{D}(b)\kappa \geq c_*(0) + \sigma_0\tilde{D}(b)\kappa \geq c_*(0)$$

Numerical approximation of the velocity

Consider the one-d version:

$$n_t = (n_x)_x - nb,$$
$$b_t = (\sigma_0 nbb_x - \chi_0\sigma_0 nb^2 n_x)_x + nb.$$

Simulations with

$$n(x,0) = n_0,\ b(x,0) = b_M e^{-x^2/6.25},$$

where $b_M = 0.71$. Underlies approximate traveling wave profile solutions for b; approximate speed can be computed from the numerical solution.

Numerical approximation of the velocity

Consider the one-d version:

$$n_t = (n_x)_x - nb,$$
$$b_t = (\sigma_0 nbb_x - \chi_0 \sigma_0 nb^2 n_x)_x + nb.$$

Simulations with

$$n(x,0) = n_0,\ b(x,0) = b_M e^{-x^2/6.25},$$

where $b_M = 0.71$. Underlies approximate traveling wave profile solutions for b; approximate speed can be computed from the numerical solution.

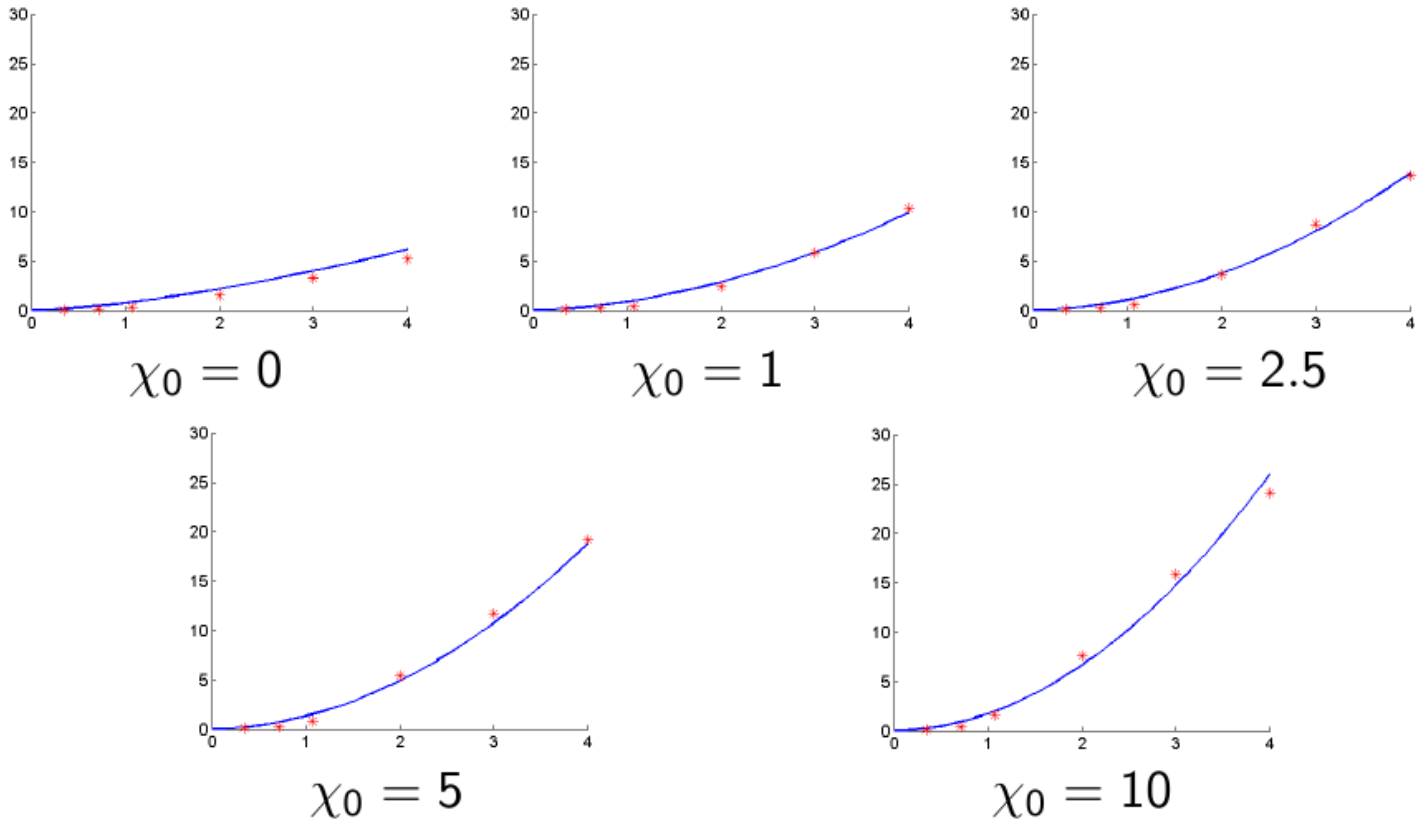

Figure: Propagation speeds vs. n_0: $*$ = numerical estimation; solid line = $2n_0\sigma_0^{1/2}\psi(b_*)^{1/2}$, $\sigma_0 = 1$

Scheme

- Square domain $[0,1] \times [0,1]$. Grid of 2048 $\times$ 2048
- Finite difference, 2nd. order Runge-Kutta scheme
- Very small time steps to avoid instabilities (stiffness)
- Compensated by parallel high performance computations with 100s of processors in Graphic Processing Units (GPUs)
- Millions of steps in a few hours.
- NVIDIA Tesla© C2070 graphics card with 448 CUDA cores

Parameter values:

Description	Symbol	Values
Initial condition for the nutrient	n_0	1.07, 0.71
Agar softness	σ_0	1.0, 4.0
Chemotactic signal strength	χ_0	0, 2.5, 5.0, 7.5, 10.0

Initial condition (Kawasaki):

$$b_0(x,y,0) = b_M e^{-(x^2+y^2)/6.25}, \qquad b_M = 0.71.$$

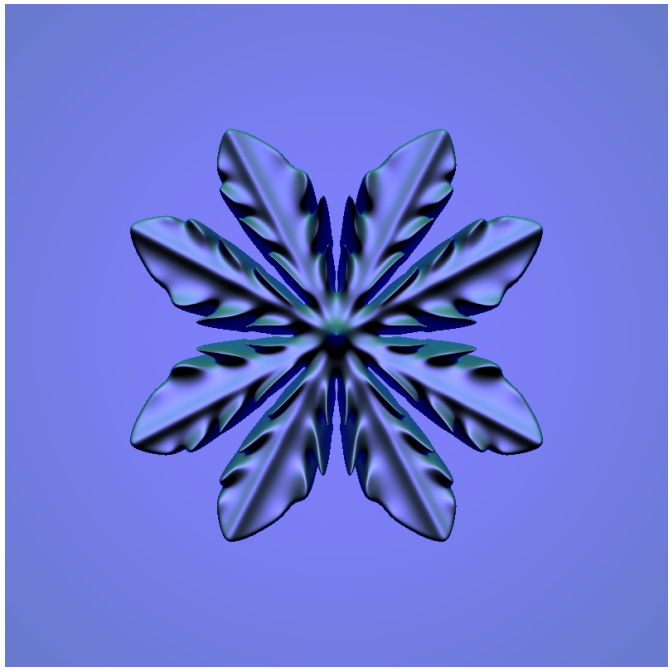

Figure: Simulations with $n_0 = 0.71$, $\chi_0 = 5$, no random fluctuations $\Delta = 0$ ($\sigma = \sigma_0 = 1$); grid of 2048×2048. High degree of symmetry due to the implicit anisotropy of the grid.

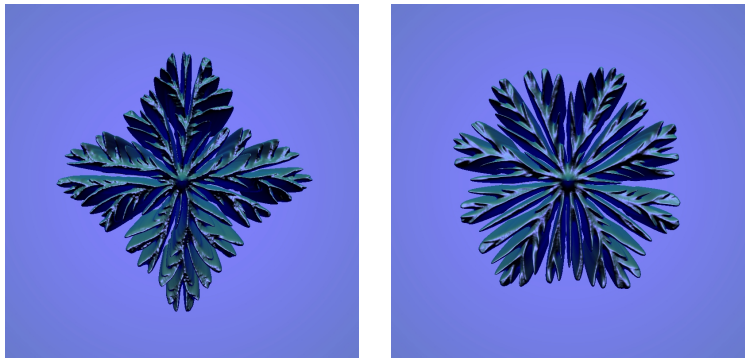

(a) 1024×1024 (b) 2048×2048

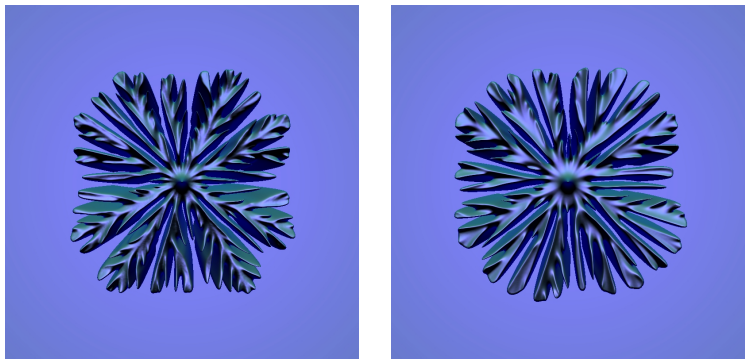

(c) 4096×4096 (d) 8192×8192

Figure: Simulations with $\sigma_0 = 1, n_0 = 0.71$ and $\chi_0 = 5$, $\Delta \neq 0$.

Semi-solid agar: $\sigma_0 = 1$; low-nutrient $n_0 = 0.71$.

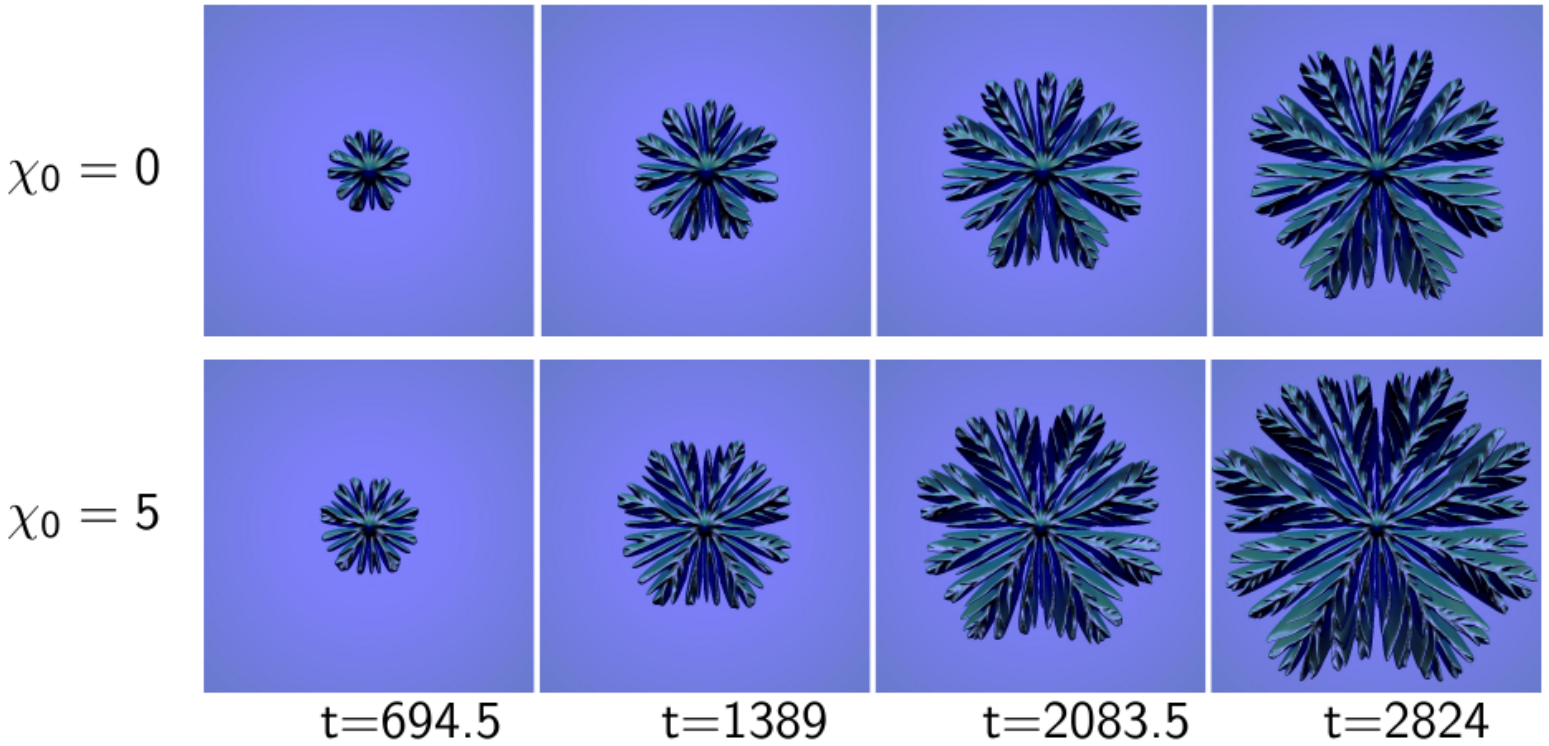

Semi-solid agar: $\sigma_0 = 1$; medium-nutrient $n_0 = 1.07$.

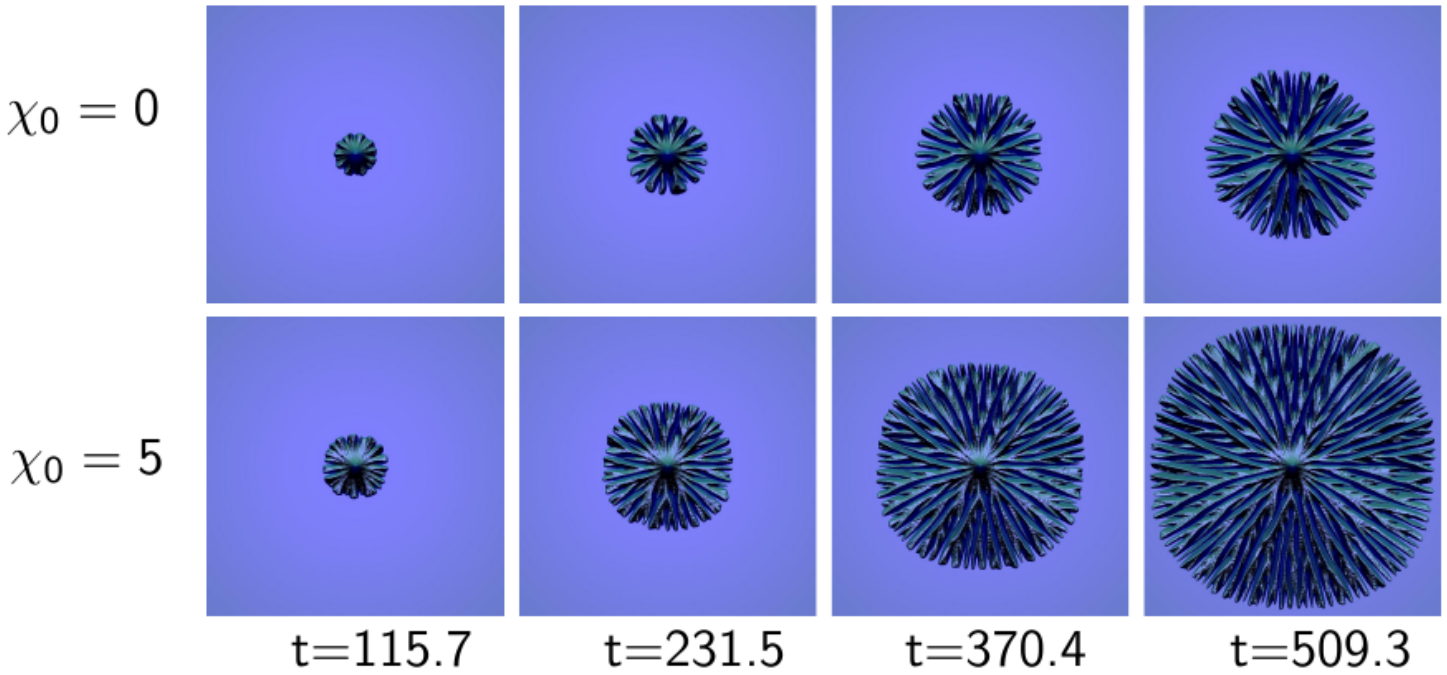

Soft agar: $\sigma_0 = 4$; low-nutrient $n_0 = 0.71$.

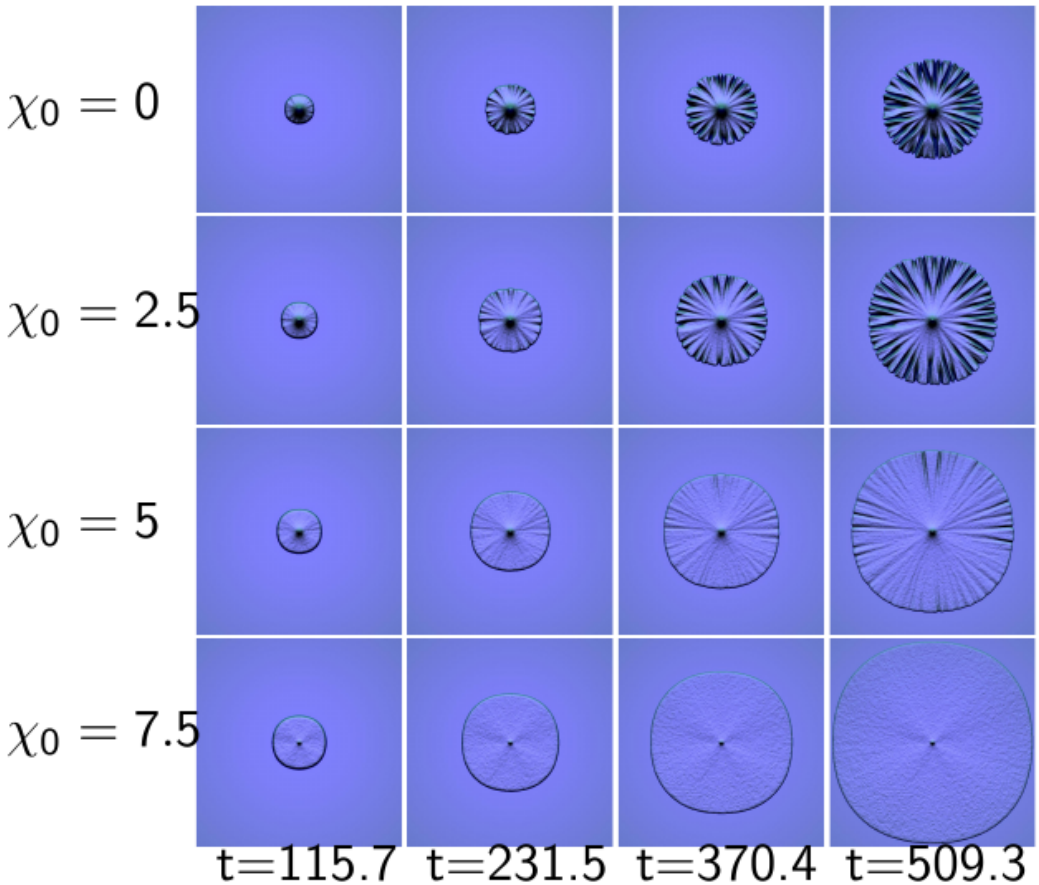

Soft agar: $\sigma_0 = 4$; med-nutrient $n_0 = 0.71$.

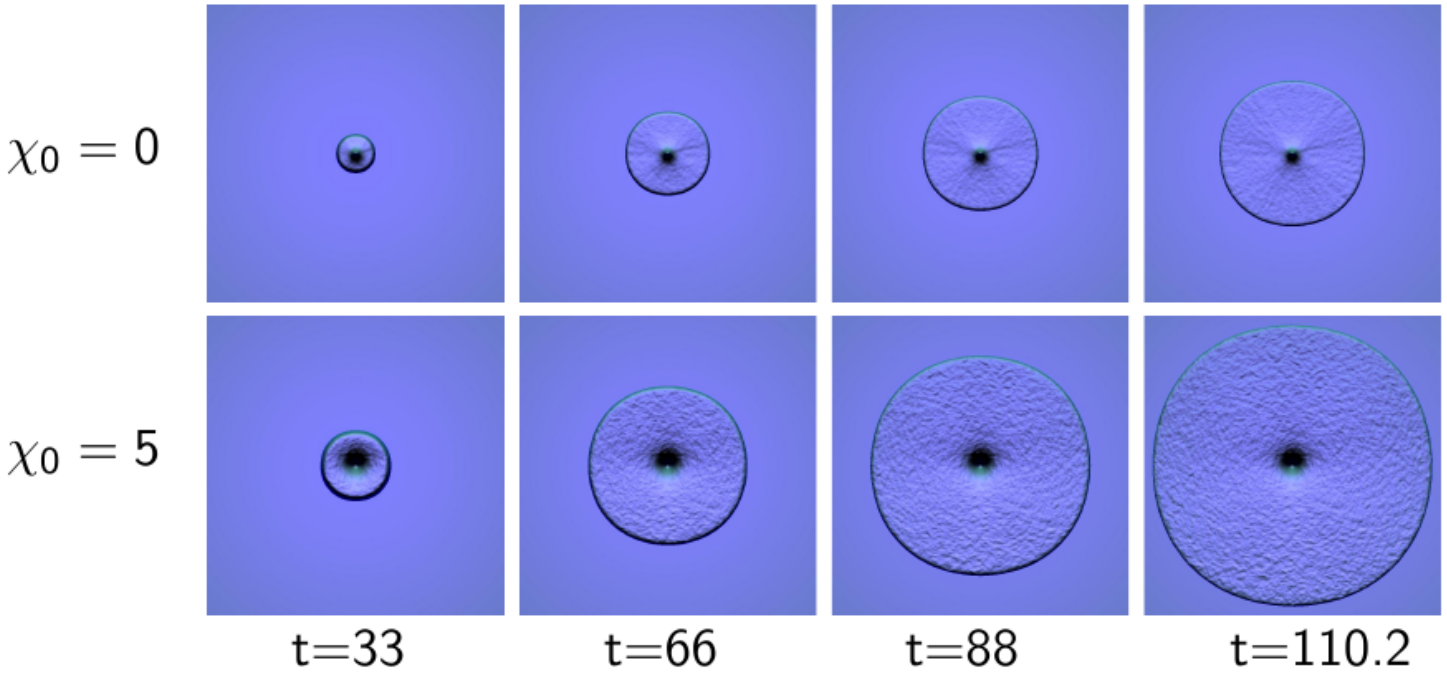

Discussion

- Incorporation of a suitable chemotactic term to Kawasaki's nonlinear cross diffusion model
- Compatible with low-nutrient regime experimental observations (Ben-Jacob)
- Asymptotics show that the speed of the envelope front increases with chemotaxis
- Numerical estimation (one-d simulation) approximates well the asymptotic speed calculation
- High resolution numerical simulations confirm enhancement of the speed
- In the low-nutrient, soft-agar regime: change in morphology, patterns become smoother (less branches) in the presence of chemotaxis

Instability vs. front speed

Transition **(E)** to **(D)**. Effect of chemotaxis supresses the onset of instability (formation of branches). Morphology gets homogeneized. Still, speed of front increases.

- Arouh, Levine, *Phys. Rev E.* **62** (2000): for Kessler-Levine RD equations, add nutrient chemotaxis. Reflected in the decrease of the "growth rate" of the perturbation of the envelope: supress instability. Calculation can be extrapolated to other models.

"....Why does chemotaxis suppress the onset of the instability, especially inasmuch as a naive analysis might lead one to argue that chemotaxis causes outwardly protruding parts of the colony to move faster as they feel higher gradients?"

Instability vs. front speed

Transition **(E)** to **(D)**. Effect of chemotaxis supresses the onset of instability (formation of branches). Morphology gets homogeneized. Still, speed of front increases.

- Arouh, Levine, *Phys. Rev E.* **62** (2000): for Kessler-Levine RD equations, add nutrient chemotaxis. Reflected in the decrease of the "growth rate" of the perturbation of the envelope: supress instability. Calculation can be extrapolated to other models.

"....Why does chemotaxis suppress the onset of the instability, especially inasmuch as a naive analysis might lead one to argue that chemotaxis causes outwardly protruding parts of the colony to move faster as they feel higher gradients?"

Reference:

- Leyva, Malaga, P, *Phys. A* **392** (2013), 5644-5662.

Thank you!